The direct and interactive impacts of hydrological factors on bacillary dysentery across different geographical regions in central China

Shudi Zuo [a], Lianping Yang [b,*], Panfeng Dou [a], Hung Chak Ho [c,d], Shaoqing Dai [e], Wenjun Ma [f], Yin Ren [a], Cunrui Huang [b,g,h,i]

[a] Key Laboratory of Urban Environment and Health, Institute of Urban Environment, Chinese Academy of Sciences, Xiamen, China
[b] School of Public Health, Sun Yat-sen University, Guangzhou, China
[c] Department of Urban Planning and Design, The University of Hong Kong, Hong Kong
[d] School of Geography and Remote Sensing, Guangzhou University, Guangzhou, China
[e] Faculty of Geo-Information Science and Earth Observation (ITC), University of Twente, Enschede, Netherlands
[f] Guangdong Provincial Institute of Public Health, Guangdong Provincial Center for Disease Control and Prevention, Guangzhou, China
[g] Shanghai Typhoon Institute, China Meteorological Administration, Shanghai, China
[h] Shanghai Key Laboratory of Meteorology and Health, Shanghai Meteorological Service, Shanghai, China
[i] School of Public Health, Zhengzhou University, Zhengzhou, China

HIGHLIGHTS

- Hydrological factors from InVEST were firstly explored on bacillary dysentery (BD).
- Hydrological factors significantly affected BD in plain, hilly, mountainous regions.
- The quick flow dominated the BD incidence in the plain and hilly regions.
- The impact factors for mountainous region were complex.
- Baseflow & local recharge strongly interacted with socioeconomic & weather factors.

GRAPHICAL ABSTRACT

The individual influence of the factors on the bacillary dysentery case number in three different regions and in Anhui province, China (left); The top 10 pairs interaction of the hydrological factors with the other factors (right).
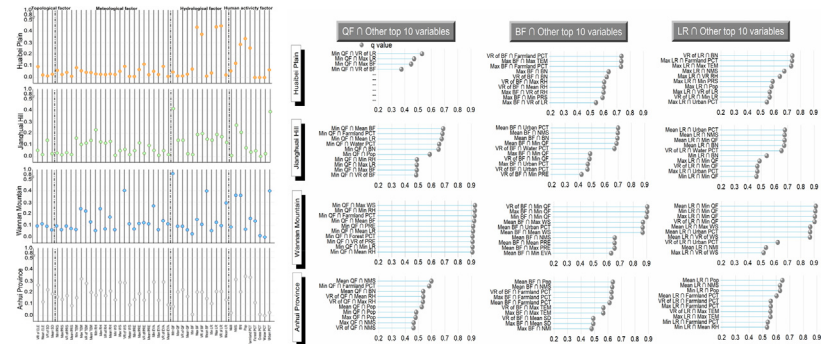
ARTICLE INFO

ABSTRACT

Previous studies found non-linear mutual interactions among hydrometeorological factors on diarrheal disease. However, the complex interactions of the hydrometeorological, topographical and human activity factors need to be further explored. This study aimed to reveal how hydrological and other factors jointly influence bacillary dysentery in different geographical regions. Using Anhui Province in China, consisted of Huaibei plain, Jianghuai hilly and Wannan mountainous regions, we integrated multi-source data (6 meteorological, 3 hydrological, 2 topographic, and 9 socioeconomic variables) to explore the direct and interactive relationship between hydrological factors (quick flow, baseflow and local recharge) and other factors by combining the ecosystem model InVEST with spatial statistical analysis. The results showed hydrological factors had significant impact powers (q = 0.444 (Huaibei plain) for local recharge, 0.412 (Jianghuai hilly region) and 0.891 (Wannan mountainous region) for quick flow, respectively) on bacillary dysentery in different regions, but lost powers at provincial level. Land use and soil properties have created significant interactions with hydrological factors across Anhui province. Particularly, percentage of farmland in Anhui province can influence quick flow across Jianghuai, Wannan regions and the whole province, and it also has significant interactions with the baseflow and local recharge across the

* Corresponding author at: School of Public Health, Sun Yat-sen University, No.74, Zhongshan 2nd Road, Guangzhou 510080, China.
  E-mail address: yanglp7@mail.sysu.edu.cn (L. Yang).

plain as well as the whole province. Percentage of urban areas had interactions with baseflow and local recharge in Jianghuai and Wannan regions. Additionally, baseflow and local recharge could be interacted with meteorological factors (e.g. temperature and wind speed), while these interactions varied in different regions. In conclusion, it was evident that hydrological factors had significant impacts on bacillary dysentery, and also interacted significantly with meteorological and socioeconomic factors. This study applying ecosystem model and spatial analysis help reveal the complex and nonlinear transmission of bacillary dysentery in different geographical regions, supporting the development of precise public health interventions with consideration of hydrological factors.

1. Introduction

Diarrheal disease driven by a variety of pathogens is one of several global health problems that is unlikely to be solved by economic development in the near term (WHO, 2014), accounting for 10–12% of all deaths in children under five years old, and an estimated 1.57 million deaths worldwide in 2017 (GBD 2017 Causes of Death Collaborators, 2018; Levy et al., 2016). The transmission and the dynamics of the pathogens causing the diarrhea varies together with land surface environmental, meteorological, sociocultural and economic factors. With the global climate change, the change in the water cycle and the hydrological conditions has the potential to severely impact the diarrheal disease (IPCC, 2014). Local health care professionals have perceived the higher risks of emerging and re-emerging infectious diseases within the changing climate and environment; however, they felt that insufficient knowledge about the driving factors on the common infectious diseases (Yang et al., 2020). Understanding the impact of the complex phenomena of earth system on enteric diseases is critical for the prediction of risks and the adoption of the prevention and intervention measures. On the basis of recognizing the direct factors influences the enteric infectious diseases, there has been call for further research to identify the potential hydrological factors and their interactions with the other factors across different divisions characterizing typical geographical features (Colston et al., 2019).

Bacillary dysentery caused by *shigella* species is one of the causes for the acute diarrheal disease. Since there is no effective vaccine, the prominent popularity due to the flood or severe rainfall events has attracted the scholars' attentions (Liu et al., 2016; Zhang et al., 2016). Besides the factors of precipitation, the other meteorological factors (e.g., temperature, relative humidity, air pressure, evaporation), topographical factors (e.g. altitude, land use) and socio-economic indicators (e.g. access to water, index of poverty, age, education, human mobility) were also considered in the water borne disease's analysis at various temporal and spatial scales (Lo Iacono et al., 2017). Two main clusters of methods including the process-based models (PBM) described by mechanistic compartmental models and the time-series & spatial epidemiological methods (TS-SE) were used (Lo Iacono et al., 2017). Despite the pathogenic principle is clear, the identification of the pathway of the transmission is always a major concern (Wang et al., 2019). Because the microbial dynamics, the spread of the pathogen through the environment, and host factors and behaviors are determined by the interaction of the hydrological, sedimentary and exposure processes (Alexander et al., 2018).

The lack of the adequate characterization of these processes not only results in the inconsistent analysis result, also hampers the ability to address the population vulnerabilities. For example, the rainfall significantly correlated with the number of dysentery cases and affected the transmission of it in China in terms of the cases data of the period 1987–2000 (Zhang et al., 2008). Liu et al. (2016) found that the flood significantly increased the risks of bacillary dysentery. However, the studies conducted in rural Bangladesh and Qingdao, China found that the flood didn't alter the risk of diarrhea (Milojevic et al., 2012; Zhang et al., 2016). Around 60%–70% multiple studies investigated the relationship between the flood and precipitation variables with the water borne diseases were positive (Levy et al., 2016). This indicated that

the potential link of the pathway might be ignored. Although there was a recent cohort study combined the meteorological and the hydrological variables together to model and predict rotavirus infection (Colston et al., 2019). It only took the total surface runoff as the hydrological variable, but lacked the consideration of the underground and long-term hydrologic cycle. Furthermore, the interactions of the nine hydrometeorological variables were assessed, but the geographical and human activity factors were still absent.

Therefore, this study explored the direct and the interactive impacts among the various hydrological, topographical, meteorological and human activity factors on the bacillary dysentery cases of Anhui Province, China in 2015 applying the spatial statistical method. The investigation would be carried out in three geographical divisions representing the plain, hilly and mountainous terrain respectively, to have the deep insights on the diversity of the complex interactions under the homogeneous climate and geographical characteristics. With the focus of the short- and long-term hydrological variables, our research fills in the literature gap, by providing explorative evidence-based of the associations between the hydrological process and bacillary dysentery disease, and favoring the more credible assessment on risk associations of exposures.

2. Data and methodologies

To quantify the drivers for the bacillary dysentery dynamics which are closely coupled with the hydrometeorological, topographical and anthropic variables across the aquatic-terrestrial interface, the Geodetector model was used to measure the direct and interactive impact powers of the hydrological variables (Wang et al., 2010; Wang et al., 2016; Wang and Xu, 2017). This method takes the spatial configuration and composition of landscape into account and evaluates the similarity and causal relationship among the geographical objects. The ecosystem service evaluation model – Integrated Valuation of Ecosystem Services and Tradeoffs (InVEST) was adopted to evaluate the hydrological variables in order to help understand the hydrological processes in the year, in particular the partition between quick flow (include runoff, interflow and direct precipitation), baseflow (the longer-term discharge derived from natural storages) and local recharge (Hamel et al., 2020; Sharp et al., 2015).

2.1. Study region

Anhui province (114.9–119.6 E°, 29.4–34.6 N°) is located in the central China, with the Yangtze and Huai Rivers running through its hinterland. The province (140,100 km^2) has 105 counties/districts, including a population of 61.43 million in 2015. The terrain of the province is high in the southwest and low in the northeast. According to the topography and natural environment, the province can be divided into three geographical divisions: Huaibei plain, Jianghuai hilly and Wannan mountainous region (Anhui Provincial Government, 2013). The plain area accounts for 45%, while the hilly and mountainous area accounts for 55% of the whole province. The four distinct seasons, which is characterized by warm and fickle spring and concentrated rainy summer, dominate the precipitation. Huaibei (The north of Huai River) plain has a warm temperate semi-humid monsoon climate. In the south of Huai

River, there are mainly subtropical humid monsoon climate. The Huaibei plain and Jianghuai hilly regions are the traditional grain production areas in China. In 2015, the annual average temperature was 16.2 °C and the annual precipitation was 1386 mm, nearly 20% higher than that of the common situation (Anhui Climate Center, 2015). During the plum rain season (24th June-25th July), because of the intense rainstorms, the flash floods occurred in Chu River basin in the east of the Jianghuai hilly region and Dabie mountain area in the west of Jianghuai hilly region. There was heavy rainfall in the Wannan mountainous region as well. The annual incidence rate of bacillary dysentery in Anhui province fluctuated from 10.26/100 thousand to 29.13/100 thousand in 2004–2017 years, with an annual incidence rate of 19.55/100 thousand (J. Zhang et al., 2019). Specifically, Anhui province's incidence rate of bacillary was 15.8/100 thousand in the year of 2015, which was higher than national incidence rate of 10.11/100 thousand. High incidence rate was found in densely populated areas, such as northern Anhui province and Hefei city.

According to local topography, Huaibei plain region is mainly covered by a northwestern side of watershed of the middle reach of the Huai River with a pinnate parallel and typical floodplain river network over 30 counties/districts. Jianghuai hilly region characterizing dendritic river network and the transition from plain to mountain has 40 counties/districts covering both southeastern side of middle reach of the Huai River's watershed and a part of the Yangtze River's watershed which faces northwest, including 19 counties/districts in the Dabie Mountains. Wannan mountainous area of Southern Anhui and covering a part of the Yangtze River's watershed facing southeast with a dendritic pattern catchment across 35 counties/districts (Fig. 1). Hefei as the capital of Anhui Province locates in the central part of the Jianghuai hilly region and has the highest GDP (566.03 billion yuan) and second highest capita GDP in the province. Wuhu city only accounting for the half GDP of Hefei city ranks the second, followed by Maanshan city accounting for only one forth GDP of Hefei city (Anhui Provincial Bureau of Statistics, 2016).

2.2. Data sources and pre-processing

The anonymous individual incidence data of bacillary dysentery disease was from the National Disease Surveillance System (NDSS), and all the infected cases were clinically confirmed (Fig. 2). According to the National Law on Infectious Diseases Control, once every case of infectious diarrhea was confirmed, it should be reported to the local health department, which must then update the information within 24 h in the public health system. Therefore, compliance dimension of disease notification was consistent over the period of our study. Disease data was provided by the Anhui Provincial Center for Disease Control and Prevention of China, and ethical approval for the study was achieved from the Ethics Review Board of School of Public Health, Sun Yat-sen University, China. The data we obtained were recorded uniformly by county/district administrative code. Therefore, there was no accurate information of the patients' addresses.

We quantified the following annual total hydrological variables at 1 km resolution using simulation results from the Seasonal Water Yield module (SWYM) of InVEST in 2015: Baseflow (BF); Local recharge (LR); and Quick flow (QF) which is the sum of the 12 monthly QFs. The outputs of the module represent the aquifer hydrological dynamic that underline the short-term surface and long-term groundwater water resources. For example, we use the yearly quick flow, which is also known as stormflow or direct runoff, as an indicator for surface runoff. Because rapid increases of quick flow due to the increase of surface runoff and interflow (lateral movement in the soil profile) during the rainfall event scoured and moved the surface pathogens. Meanwhile the fast-rising river height might reverse the hydraulic gradient towards the stream. Therefore, we used the baseflow and local recharge as indicators for groundwater dynamic. Since groundwater discharge from the shallow unconfined aquifer is commonly assumed to be the main contributor

to baseflow (Brodie and Hostetler, 2005). Baseflow is the portion of streamflow. In the model's output, it was only the delayed shallow subsurface flow, doesn't include the deep subsurface flow and the evapotranspirated amount before it reaches the stream. Moreover, during the dry period, the unconfined aquifer or other storages (e.g. lake, wetland…) needs to be fully replenished and has enough water to maintain the flow to the river. The local recharge represents this process contributed from upslope area.

In terms of the references, we proposed the conceptual diagram illustrating the transmission mechanisms of the water borne pathogen (e.g. bacillary dysentery) (Ding et al., 2016; Levy et al., 2016). Excepts for the flood event, there are three potential pathways for the quick flow and the baseflow to influence the pathogen transmission (Fig. 3). The first pathway of the transmission was the contamination of the drinking water by the movement of the pathogen caused by the runoff scouring. The second one modified the reason of the movement of the pathogen by the surface soil water saturation because of the precipitation and runoff. The third one was the runoff or the stream water disturbance brought out the water turbidity which results in the failure of the water treatment capacity. The fundamental cause of the infection is the contact of the contaminated drinking water which is influenced by the movement of the pathogens and the failure of the water treatment capacity (Mellor et al., 2016). The variation of the pathogens (including the location and quantity) is dominated by the interaction of the hydrological variables, the landscape pattern (land use composition), and the other geographical variables (Colston et al., 2019). Therefore, 5 land use indicators (percentages of agricultural land, forest, lawn, waterbody, the built-up area accounting for the whole county/district) and 2 topographical indicators (elevation and slope degree) were selected to measure the virus' dispersal mechanism. Besides the above variables, the socioeconomic factors (number of the medical institutes, number of the medical staff, hospital bed number, and population) were selected to measure the mediation between the primary exposure and the second transmission process. Finally, the virus survival mechanism was measured by the meteorological variables, such as pressure, temperature, relative humidity, wind speed, precipitation, and evaporation. Please see the Table 1 for all the data sources and Figs. S1–S3 for the distribution of the meteorological, topographic, socioeconomic factors (shown in the Appendix file).

The hydrological variables were the output of the SWYM of the InVEST model. The soil hydrologic group which is determined from hydraulic conductivity and soil depths were converted from Chinese standard to American standard for the suitability of the model. The study area was divided into 18 climate zones through the Tyson polygons created by the 18 meteorological stations. In terms of the observation data, we calculated the rain events for each climate zones. Biophysical table containing two parameters used for the calculation of the quick flow and evapotranspiration. The curve number (CN) was tabulated as a function of the local LULC, and soil group. The Kc used to calculate the potential evapotranspiration (PET) is the vegetation coefficient which could be obtained by the leaf area index (LAI). The values of CN and Kc were guided by the manual of InVest software (Sharp et al., 2015). Please see the Table 2 for descriptions of all the input data. Explanations of each of the parameters can be found on the website (http://data.naturalcapitalproject.org/nightly-build/invest-users-guide/html/seasonal_water_yield.html).

2.3. InVEST SWYM description and the accuracy assurance

InVEST is a toolset including various models for quantifying, mapping, valuing the benefits provided by the ecosystem. In this study, we used the version 3.7.0. The SWYM simulates the hydrological process in the catchment. In this model, the quick flow represents the generation of streamflow with watershed residence times of hours to days. The baseflow is defined as the contribution of a pixel to slow release
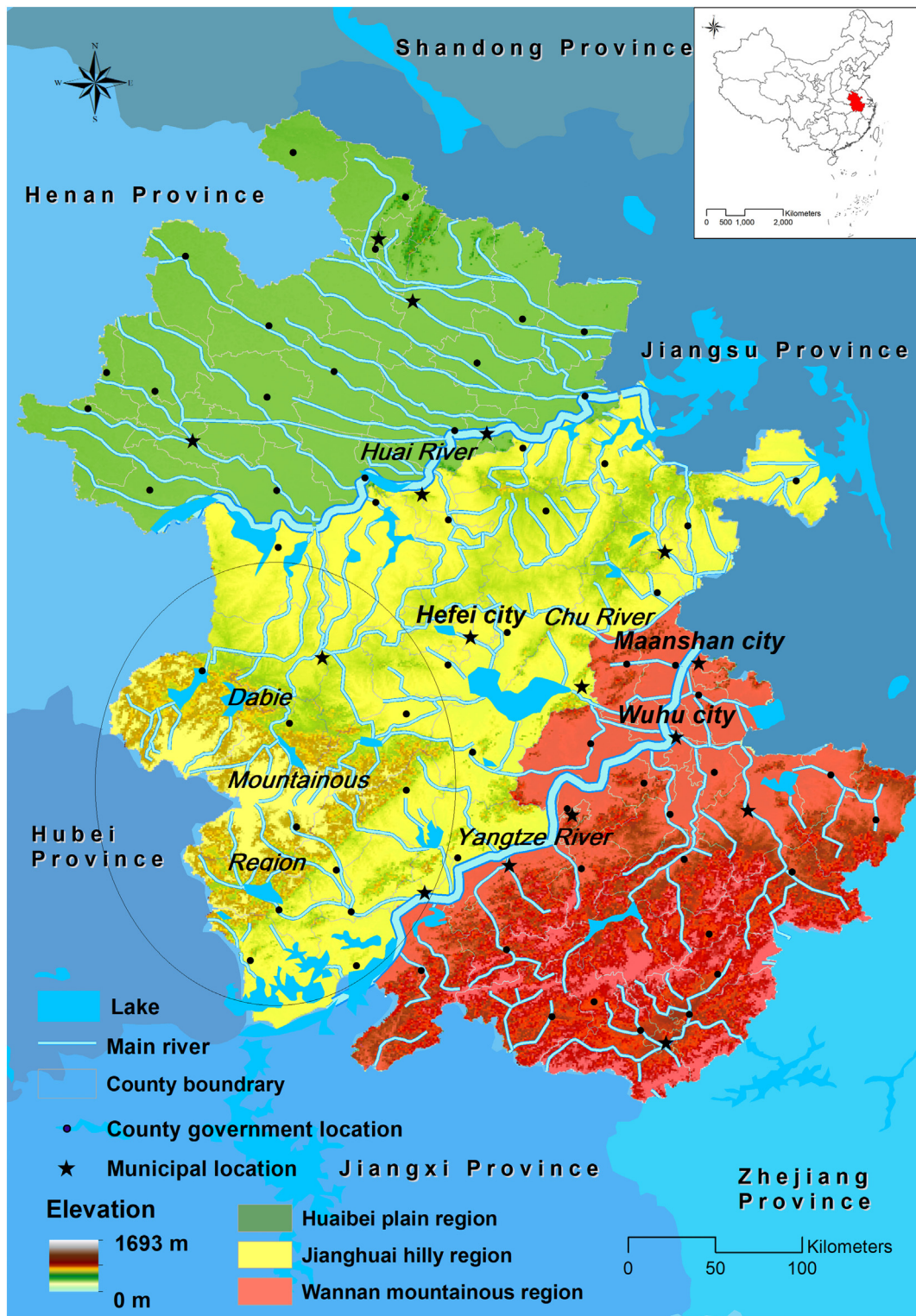
Fig. 1. The location of Anhui province by geographical regions.

flow in the model. The local recharge map used in this study refers to the available quantities which could flow out from this pixel.

Based on the Curve Number (CN) approach (Fangmeier et al., 2005), where the model uses the mean event depth, the precipitation of each rain events at a given pixel, and assumes an exponential distribution of daily precipitation depths on days with rain to calculate the quick flow. The curve number is an experience coefficient capturing the soil and land cover properties. The higher values of CN have higher runoff potential (e.g. clay soils and low vegetation cover), lower values are more likely to infiltrate (e.g. sandy soils and dense vegetation cover). However, the quick flow for pixels located in streams is set to the precipitation on that pixel, which assumes no infiltration, only runoff. The module calculated the monthly QFs values as the intermediate outputs and then sum them up to export the annual quick flow (QF) as the final output.
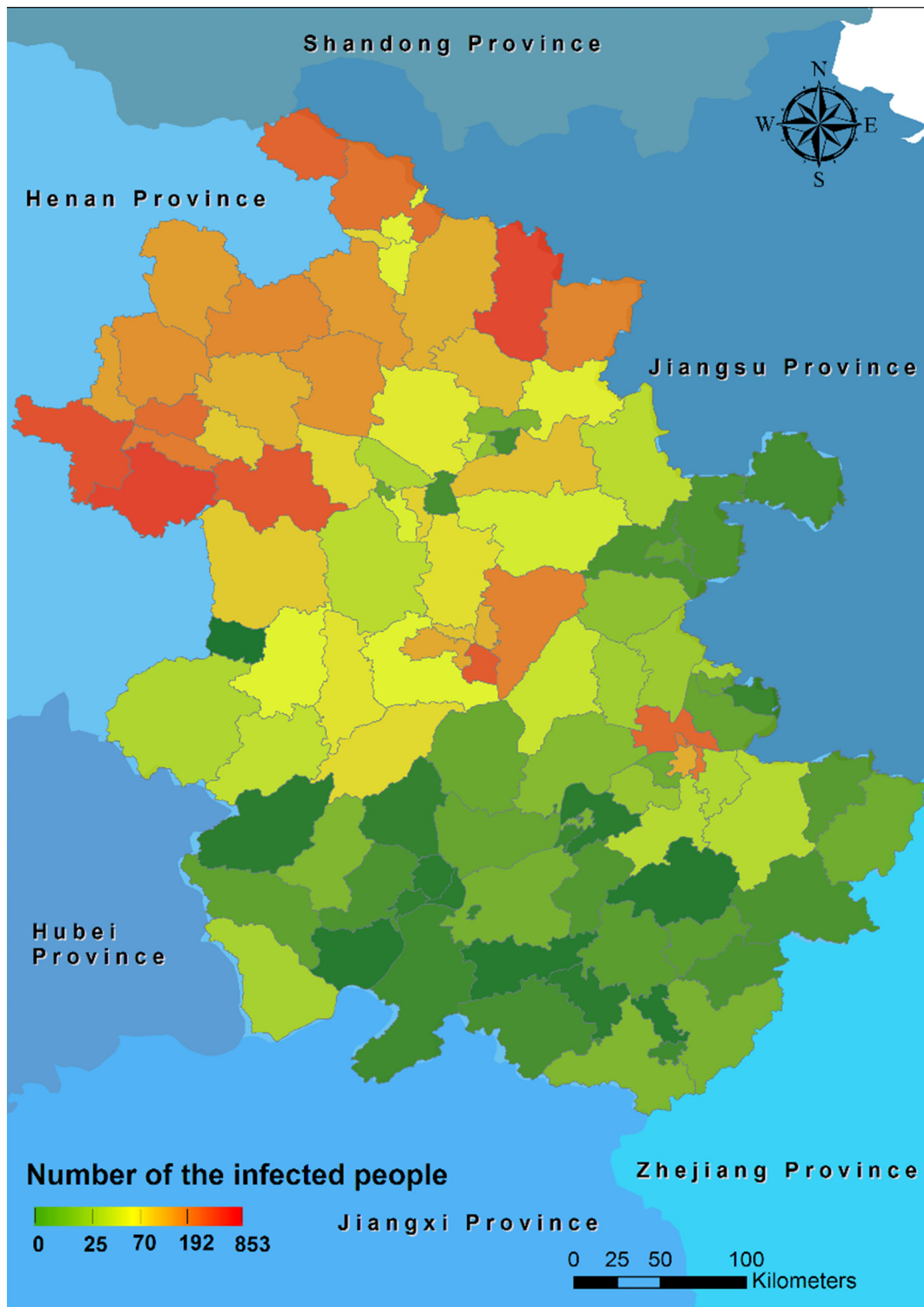
Fig. 2. Distribution of bacillary dysentery cases across Anhui province, 2015.

Precipitation infiltrate the soil to become local recharge, which can be negative if a raster pixel does not receive enough water to satisfy its vegetation requirements (determined by Kc). Therefore, the water generated upslope of the pixel was calculated as the baseflow of this pixel which is a function of the amount of flow leaving the pixel and of the relative contribution to recharge of this pixel. The negative local recharge represents the zero baseflow. The annual local recharge was the accumulation of the monthly water budgets.

We applied two ways to ensure the simulation accuracy. Firstly, since the meteorological parameters are the sensitive input parameters of the seasonal water yield module (Sahle et al., 2019). We compared the spatial interpolation methods, such as the inverse distance weighted (IDW), Kriging, radial basis functions (RBF), global polynomial interpolation (GPI), interpolation with barriers (IWB) through the "leave-one-out cross validation" and found that the optimal interpolation method for precipitation (172.23 mm) and evapotranspiration
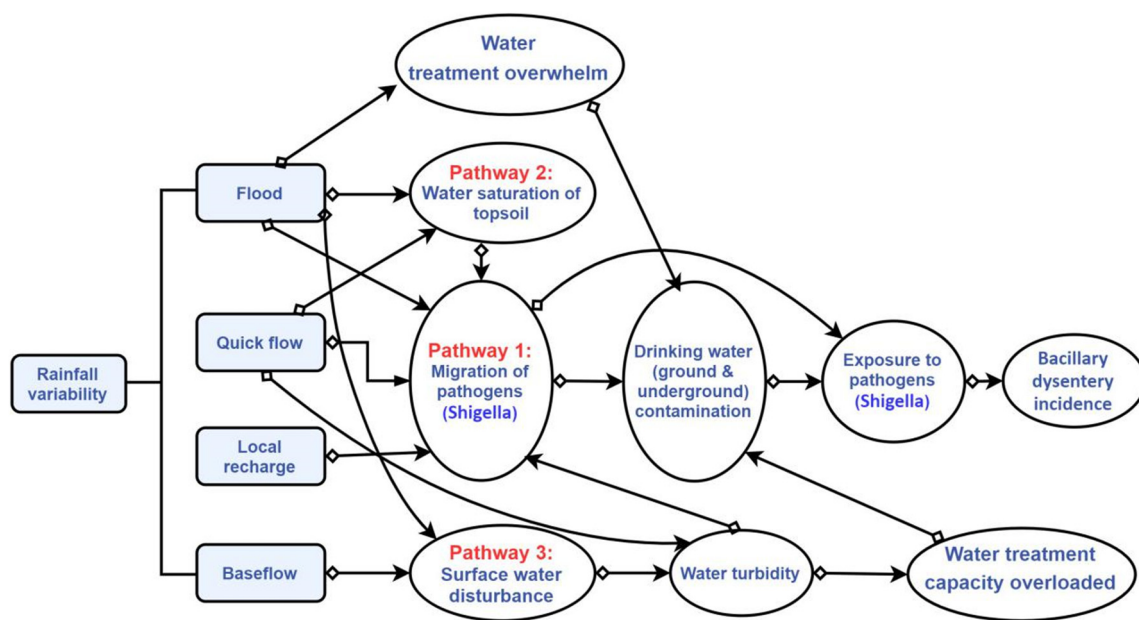
Fig. 3. The conceptual diagram illustrating the relationship between bacillary dysentery and hydrological factors.

(87.22 mm) was the Kriging method of which the root mean square error (RMSE) between the predicted and observed values was the smallest among all the other methods. Please see the appendix table S1 and S2 for detail information. Secondly, since the flow accumulation threshold (TFA) controlled the density of the river network (Redhead et al., 2018), we calibrated it by comparing the real and the simulated regional river map.

Table 1
The geographical, hydrometeorological, socioeconomic variables, data feature and sources.

Type	Variable	Data feature
Hydrological	Baseflow, BF Local recharge, LR Quick flow, QF	1 km grid raster data, with the unit mm/km^{-2} Three variables were the output of the InVEST model.
Topographical	Elevation, ELE Slope degree, SD	1 km grid raster data, with the unit m. Derived from Digital elevation model (DEM) data, with the unit degree.
Meteorological	Mean Pressure, PRS Mean Temperature, TEM Mean Relative humidity, RH Mean Wind speed, WS Total Precipitation, PRE Total Evapotranspiration, EVA	1 km grid raster data were interpolated by the Kriging method in terms of the station observation data, with the unit hPa, °C, %, m/s, mm, mm respectively.
Socioeconomic	Land use/land cover, LULC	The proportion of 5 different land use types in each county, including agricultural land, forest, lawn, and construction land percentage was from the Resource and Environment Science Data Center, Chinese Academy of Sciences (http://www.resdc.cn).
	Number of the medical institutes, NMI Number of the medical staff, NMS Bed number, BN Population, POP	The statistics data for each county/district from the 2016 China Cities Statistical Yearbook.

2.4. Multiple source data integration and Geodetector model

2.4.1. Multiple source data integration

According to the literature investigation, we selected 4 categories of variables consisted of the statistical and raster data as the factors affecting the incidence of bacillary dysentery. We used the correcting and conversion methods (e.g., resampling, coordinate transformation, and geometric correction) on different types of data to build the multi-source dataset with the uniform coordinate projection system. After obtaining the spatial distribution of 6 meteorological variables, 3 hydrological variables and 2 topographic variables, based on the county/district administrative boundaries, we used the zonal statistics function of Arcmap 10.1 to calculate the average, variation range, minimum and maximum values for each county/district. Then the case numbers and the 9 socio-economic variables including 5 land use type percentages indicators and the 4 indicators for the sanitary and medical services conditions from the statistical yearbook of each county/district were combined with the other variables. After this step, the final input data of Geodetector model was prepared. Each counties/districts of this dataset had the attributes including topography, meteorology, hydrology and human activity. Since the Geodetector method could be used to analyze category variables (Zuo et al., 2018). The Jenks natural breaks classified method (Dent, 1999) was applied to the continuous variable in order to meet the strata requirement of the model.

2.4.2. Geodetector model

The spatial heterogeneity is one of characteristics of the geographical objects. When the sum of the variances of each strata is less than the sum of the variances of the whole research area, the stratified heterogeneity exists. The similarity of the spatial distribution of the two variables (e.g. case number vs quick flow) which could be measured by the Geodetector model demonstrated the causal relationship. Since the lack of the exact the address and the mobile trajectory of the patients, the dependent variable of our study is the case number of the county/district which conforms to the stratification premise of the Geodetector.

In terms of the three geographical divisions, the output (q) of the factor detection of Geodetector was used to analyze the influence of the individual factor to the spatial distribution of case numbers, and the p value of F test was used to determine the significance level

Table 2

The parameters and the input data of the Seasonal Water Yield module.

Parameters and input data	Data sources	Data description and preprocess	Units
Monthly precipitation	The China Meteorological Data Service Center (CMDSC) (http://data.cma.cn)	The average monthly precipitation station data were interpolated by the Kriging to get the raster dataset without the default values.	1 km resolution
Monthly ET$_0$ (evapotranspiration)	The CMDSC (http://data.cma.cn), Kriging interpolation	The average monthly evapotranspiration data calculated by Penman-Monteith formula were interpolated by the Kriging to get the raster dataset without the default values (Allen et al., 1998).	1 km resolution
LULC (land use/land cover)	Resource and Environment Science Data Center, Chinese Academy of Sciences (http://www.resdc.cn)	The raster data with 6 LULC types and 25 subtypes, including agricultural land, forest, lawn, water body, construction land, and unused land.	1 km resolution
Elevation	Geospatial Data Cloud (http://www.gscloud.cn)	The DEM raster data with an elevation value for each pixel.	Resample 30 m to 1 km resolution
Soil group	Scientific Data Center for Cold and Dry Areas (http://westdc.westgis.ac.cn)	The raster data with 4 soil hydrologic groups (A, B, C, or D) was classified by the user's guide (Sharp et al., 2015).	1 km resolution
Climate zones	The China Meteorological Data Service Center (http://data.cma.cn), zoning by building Tyson polygon	The study region was divided by Tyson polygon in terms of the meteorological stations. Each polygon as the climate zone was assigned an integer code.	NA
Rain events	The CMDSC (http://data.cma.cn)	A table with monthly rainfall frequency of each climatic zone for 12 months. A rain event is defined as >0.1 mm.	Frequency
Threshold flow accumulation (TFA)	Sensitivity analysis and calibration of the model	The number of upstream cells that must flow into a cell before it is considered part of a stream.	NA
Biophysical table	Curve number (CN) and K$_c$	CN for each hydrological soil group of 25 subtypes LULC. K$_c$ for each month of 25 subtypes LULC.	NA
Calibration data	The CMDSC (http://data.cma.cn)	Station observations of the precipitation and evapotranspiration in the study region.	mm

(Wang et al., 2016; Wang et al., 2018). If the p value is less than 0.01, the double asterisk would be used to mark the q value in this study. The q value could be expressed by the equation as follows (http://www.geodetector.org/):

$$q_x = 1 - \frac{\sum_{p=1}^{m} n\sigma_{D,p}^2}{N\sigma_{D,z}^2} \tag{1}$$

where, q_X represents the influence power of each impact variable; $p = 1, 2, …, m$ is the strata of factor x; D is the potential impact factor; n and N are the number of samples in the strata and entire region respectively; $\sigma_{D,p}^2$ is the variance of the variable in the D strata; and $\sigma_{D,z}^2$ represents the variance across the study area. Assuming $\sigma_{D,z}^2 \neq 0$, the model is established. The q_x value equates to $1 - \frac{\text{sum of discrete variances}}{\text{discrete variance of population}}$. The large value indicates that the explanatory variable factor has a great influence on the explained variable. The larger the q value is, the stronger the independent variable X explains the case number, and vice versa.

In order to investigate the interaction effects from the hydrological factors and the other factors, we used the interaction detection of Geodetector. The interaction effect of Geodetector is measured by the similarity of the new variable distribution ($X_{12} = X_1 \cap X_2$) formed by intersection of variables X_1 and X_2. Then the comparison between the sum of q values of the X_1 and X_2 with that of $X_1 \cap X_2$ indicates whether the interaction between factors X_1 and X_2 increases or decreases the explanatory power of the explained variable Y, or whether the influences of these factors on Y are independent of each other. Please see the Eq. (2) for the details.

$$\left. \begin{array}{l} \text{Weaken, nolinear} - : q(X_1 \cap X_2) < \text{Min}(q(X_1), q(X_2)) \\ \text{Weaken, uni} - : \text{Min}(q(X_1), q(X_2)) < q(X_1 \cap X_2) < \text{Max}(q(X_1), q(X_2)) \\ \text{Enhance, bi} - : q(X_1 \cap X_2) > \text{Max}(q(X_1), q(X_2)) \\ \text{Indepent} - : q(X_1 \cap X_2) = q(X_1) + q(X_2) \\ \text{Enhance, nonlinear} - : q(X_1 \cap X_2) > q(X_1) + q(X_2) \end{array} \right\} \tag{2}$$

X_1 and X_2 are two selected independent variables. There are five types of the comparison results. Usually, the variable with the big single influence is the strong impact factor for the dependent Y. When the single and interactive effects of the variable are both large, it should be the dominant factor. However, the variable with the small single influence and the big interaction with the other factors needs further investigations.

3. Results

3.1. Bacillary dysentery cases profile

In 2015, 9734 infectious bacillary dysentery cases were identified in Anhui province. Among the total cases, the average age was 34.5 years old (std 28.3), and women cases accounting for 45.0%. There are 2750 cases as children under five years old (28.3%), and 1932 elders over 65 years old (19.8%).

There were obvious seasonal and geographic heterogeneity in the incidence rate (Fig. 4). The case number in Huaibei plain accounted for 63.32% of the incidence in the whole province. There were obvious
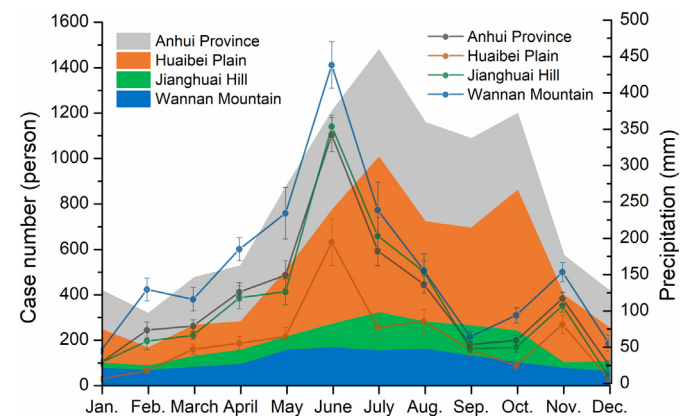

Fig. 4. The monthly case number (left axis) and the precipitation (right axis) in Huaibei plain, Jianghuai hilly and Wannan mountainous regions. (Note: The error bar of the precipitation is the standard error.)

seasonal changes, which were mainly manifested as that the incidence of the disease remained at a low level from December to April, and increased significantly from May to the first peak in July, and the second peak occurred in October. The average annual rainfall in Huaibei plain region was low, only 707.1 mm, with the peak occurring in June, August and November (Fig. 4). The case numbers of the Jianghuai hilly and Wannan mountainous areas accounted for 23.22% and 13.46%, respectively. There were certain seasonal variations with the single peak shape curve. The highest incidence was in July and June. The average annual precipitation in these two regions were 1321.6 mm and 1907.6 mm, respectively, with peaks in June and November (Fig. 4).

3.2. Hydrological factors

The spatial distribution of quick flow, baseflow and local recharge of Anhui Province in 2015 with 1 km resolution were obtained through the InVEST model (Fig. 5).The annual average of quick flows for the whole province (n = 105 counties/districts), Huaibei plain (n = 30), Jianghuai hilly (n = 40) and Wannan mountainous (n = 35) regions were 626.09 ± 253.62 (mean ± std), 406.45 ± 95.92, 584.98 ± 174.71, and 861.32 ± 228.86 mm, respectively. The annual average of baseflow for the whole province was 557.60 ± 291.82 mm. There was the largest baseflow in the Wannan mountainous region (735.07 ± 317.50 mm), flowed by the Jianghuai hilly (346.27 ± 106.52 mm) and Huaibei

plain regions (560.82 ± 261.05 mm). In the same order as the baseflow, the annual average of local recharge for the Wannan mountainous region was the largest (727.75 ± 325.78 mm), flowed by the Jianghuai hilly (548.58 ± 268.18 mm) and Huaibei plain regions (346.83 ± 105.00 mm). The local recharge for the whole province was 550.66 ± 295.44 mm.

Since the minimum values of the quick flow and the baseflow in different divisions were small which were around 1 to 10 mm. The maximum values of these two factors were similar with their variations. In terms of the boxplots, the 5%–95% range of three factors in the Jianghuai Plain region was the smallest representing that the small heterogeneity.

3.3. Individual influence of multiple factors on bacillary dysentery case number

Huaibei plain was greatly affected by the extreme value, range of hydrological factors, and human activities. For example, the main impact factors were the maximum and the variation of the local recharge (q = 0.436** and 0.444*), the maximum and the variation of the baseflow (q = 0.433** and 0.372*), population (q = 0.335*). Jianghuai hilly region was successively affected by the extreme value of hydrological factors, human activities and meteorological factors. For example, the major impact factors were minimum of quick flow (q = 0.412*), built up area percentage (q = 0.387*), minimum of relative humidity
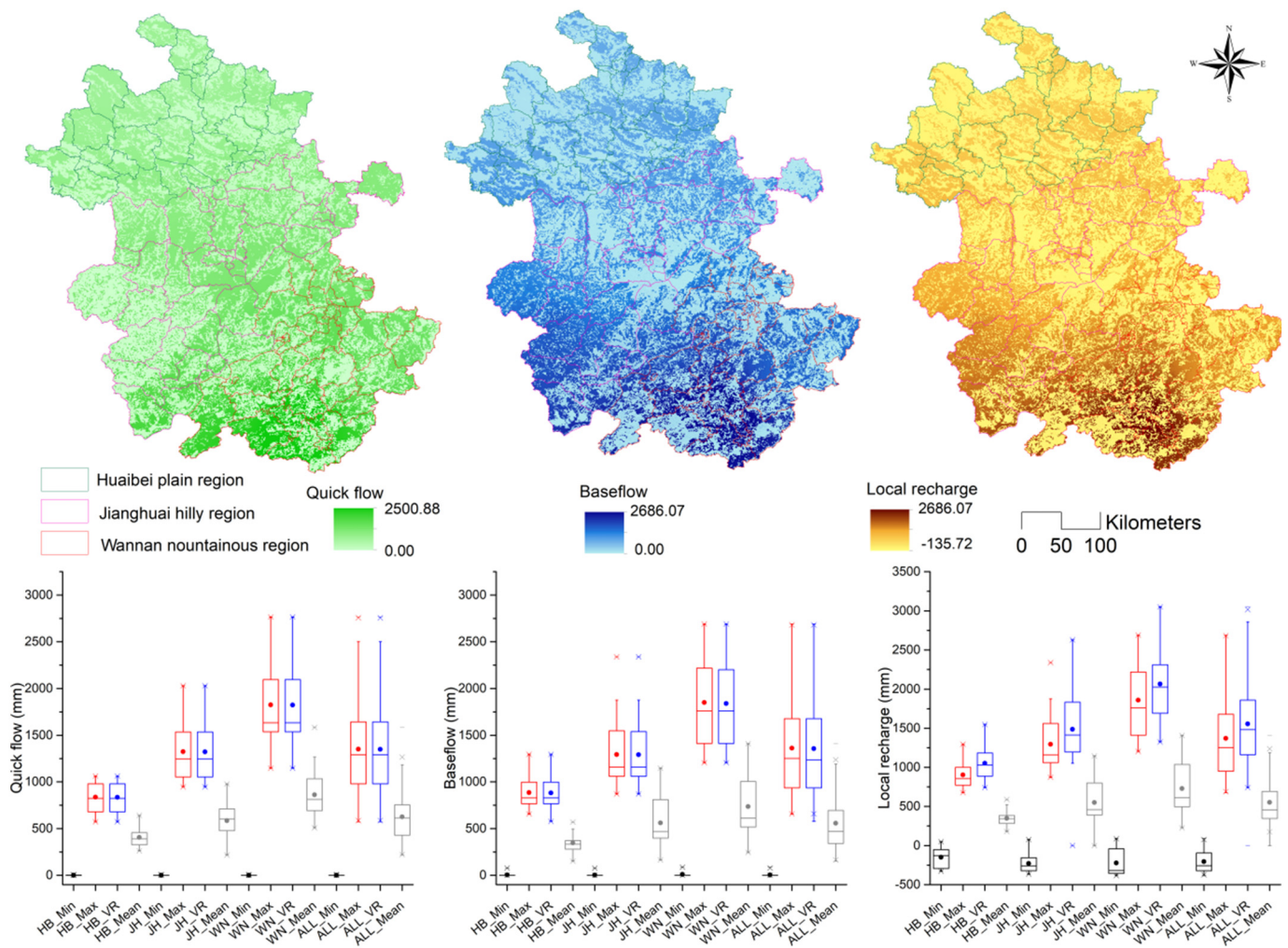

Fig. 5. Spatial distribution maps of the quick flow, baseflow and local recharge in Anhui Province. The boxplots of three hydrological factors in Huaibei plain (HB), Jianghuai hilly (JH), Wannan mountainous (WN) regions and the whole province (ALL) are shown, including the mean (dot), median, inter-quartile range (25%–75% in the box) and 5% - 95% range (whiskers). VR: variation.

(q = 0.229*). The impact factors for Wannan mountainous region were complex. While the influences of hydrological factors and meteorological factors were greater than the others. For example, the major impact factors were minimum of quick flow (q = 0.891**), maximum and variation of wind speed (q = 0.517** and 0.403**), built up area percentage (q = 0.399**), average baseflow (q = 0.398**). As to the whole province, the hydrological factors lost their influences. Because the population (q = 0.338**), agriculture land (q = 0.329**), highest temperature (q = 0.316**), the number of the medical staff (q = 0.311**), variation of evaporation (q = 0.289**) were the top five individual factors (Fig. 6, Table S3).

3.4. Interactive impacts of hydrological factors on bacillary dysentery case number

From the perspective of each region (Fig. 7, Table S4), quick flow in Huaibei plain only interacted statistical significantly with hydrological factors, while baseflow and local recharge interacted significantly with human activity factors, such as agriculture area percentages (q = 0.735** and 0.737**), hospital bed number (q = 0.624* and 0.740**), and the metrological factors, such as temperature (q = 0.734** and 0.730**). In addition to the strong interactions with other hydrological factors, the hydrological factors in the Jianghuai hilly region also had
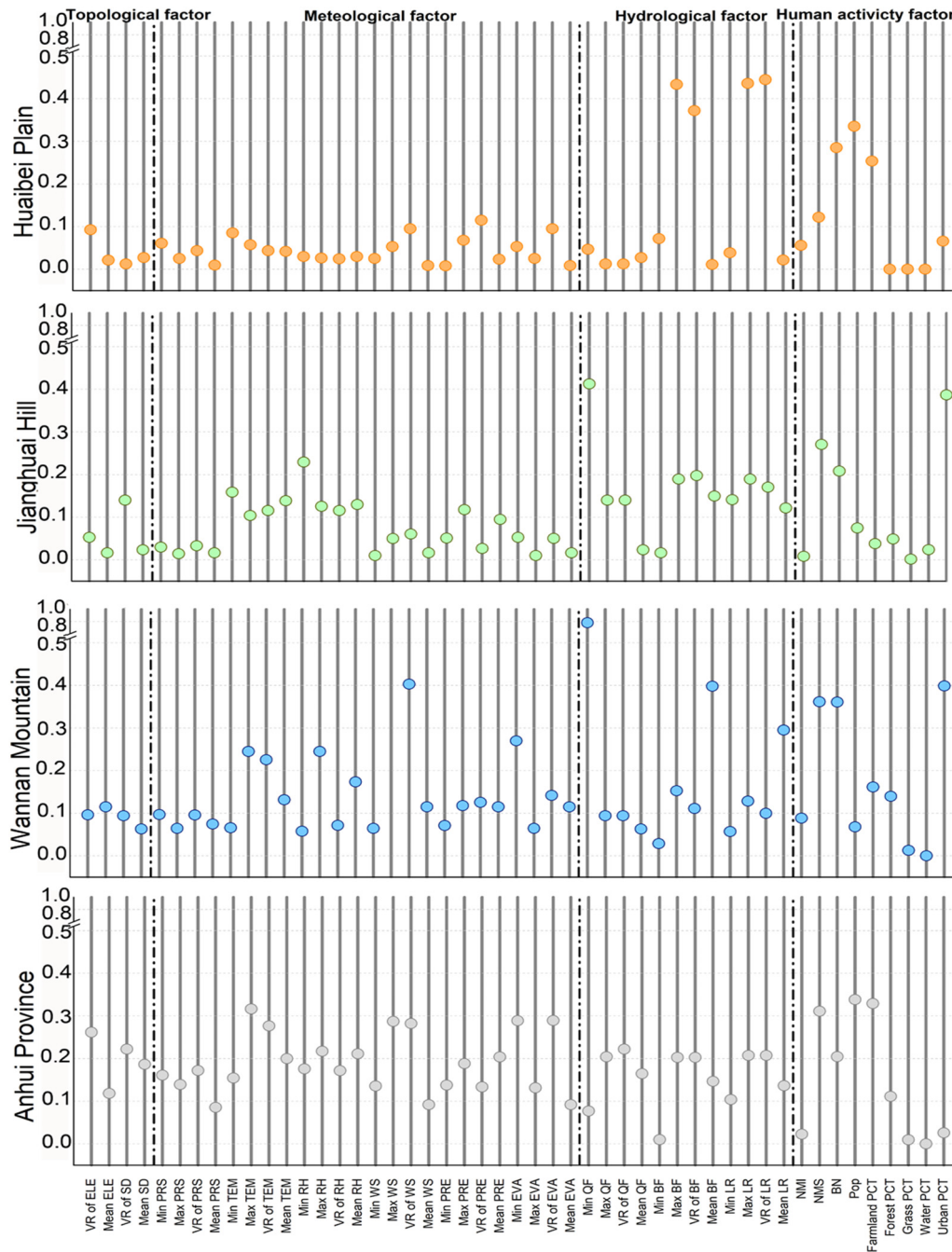

Fig. 6. The individual influence of the factors on the bacillary dysentery case number in three different regions and in the whole province. (Note: VR represents the variation of the range, ELE represents the elevation, SD represents the slope degree, PRS represents the pressure, TEM represents the temperature, RH represents the relative humidity, WS represents the wind speed, PRE represents the precipitation, EVA represents the evapotranspiration, QF represents the quick flow, BF represents the baseflow, LR represents the local recharge, NMI represents the number of the medical institutes, NMS represents the number of the medical staff, BN represents the bed number, Pop represents the population, PCT represents the percentage.)
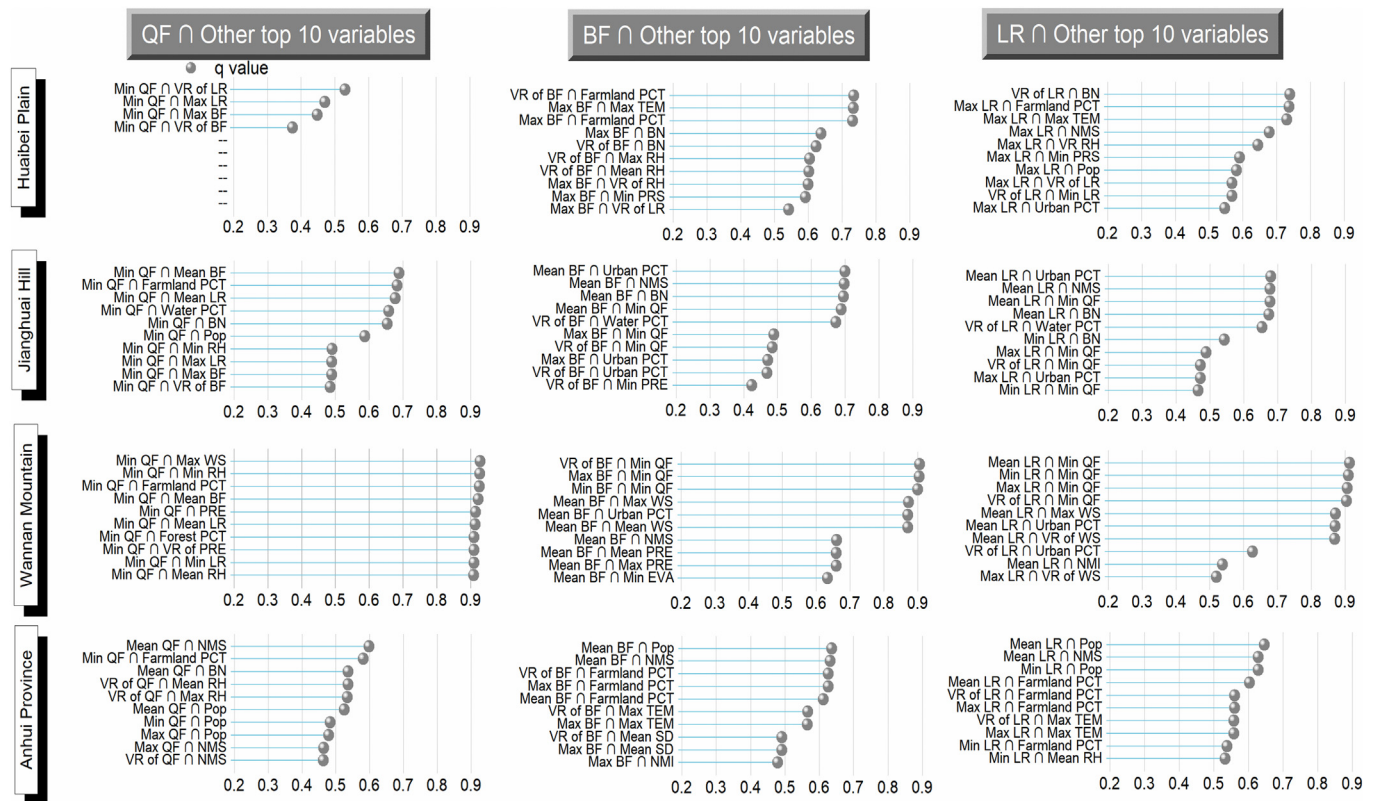
Fig. 7. The top 10 pairs interaction of the hydrological factors with the other factors (QF: quick flow, BF: base flow, LR: local recharge).

significant strong interactions with many other different factors, such as the farmland (q = 0.683*) and urban (q = 0.700** and 0.679*) percentages, which indicated that the leading factors varied greatly. The baseflow and local recharge both interacted strongly with the minimum of quick flow in Wannan mountainous region (q = 0.906** and 0.914**). Moreover, the three hydrological factors all had strong interactions with the wind speed (q = 0.929**, 0.873**, 0.872**) in Wannan region.

From the perspective of hydrological factors (Fig. 7, Table S4), quick flow interacted intensely with other hydrological factors, such as the variation of local recharge in Huaibei (q = 0.531*), mean baseflow in Jianghuai (q = 0.689*) and Wannan regions (q = 0.923**). Except for that, agriculture area percentage (0.683* in Jianghuai region and 0.926** in Wannan region) and relative humidity (0.491* in Jianghuai region and 0.928* in Wannan region) both had significant interactions with quick flow in Jianhuai and Wannan regions where the river network shape changes with the increase of the elevation. Baseflow and local recharge had the similar interaction effects on bacillary dysentery. For instance, both baseflow and local recharge had the strong interactions with agriculture area percentages in the Huaibei plain (q = 0.735** and 0.737**), with built up area percentages in the Jianghuai region (q = 0.700* and 0.679*), and with the minimum quick flow in the Wannan Mountainous region (q = 0.906** and 0.914**). But in different regions, the interactions between them and other factors varied. In the Huaibei and Jianghuai regions, they mainly interacted with human activity factors (e.g. agriculture area and built up area percentages, number of medical staff). While in the Wannan regions, they preferred the meteorological and hydrological factors (e.g. q of wind speed = 0.873** and 0.872**, q of quick flow = 0.914** and 0.906**).

From the perspective of the whole province (Fig. 7, Table S4), the interactions among hydrological factors were weaker than that of the three regions. The three hydrological factors usually had the strong interactions with the number of medical staff and the agriculture land

percentages among the human activity factors. In addition, like the Wannan regions, the interaction pattern of quick flow in the whole province had the strong interaction with the relative humidity (q = 0.537**). And baseflow and local recharge both interacted strongly with the maximum temperature (q = 0.566** and 0.558**). However, baseflow of the whole province had the similar interactions pattern with that of the Huaibei plain, which usually strongly interacted with population (q = 0.636**), agriculture land percentage (q = 0.627**), and temperature (q = 0.566**). While interaction pattern of local recharge was similar to that of the Huaibei and Jianghuai regions, which usually strongly interacted with number of medical staff (q = 0.629**), agriculture land percentage (q = 0.604**), and temperature (q = 0.558**).

4. Discussion

Although prior studies of impact factors of bacillary dysentery infectious diseases have incorporated multiple climatic, hydrological, topographical, socioeconomic variables, to the best of our knowledge, this study is the first to quantify impacts of the typical surface and underground hydrological factors together with the various factors under the consideration of the spatial landscape pattern. Since the causal relationship between climate and disease not only strictly dependents on specific ecological mechanisms associated with transmission routes, also depends on the regulation of the other secondary transmission routes (Gong et al., 2019; Kraay et al., 2018). Many environmental conditions which were influenced by the degree of country development or the natural ecological process have the complex and non-linear impacts on the pathogen community and exposure dynamics (Carlton et al., 2014; Collender et al., 2019). Our study quantified the direct and interactive impact powers of the quick-flow, baseflow and local recharge and other factors on bacillary dysentery diseases.

4.1. The single effects of hydrological factors varied in three geographical regions

We found that the impacts of the single hydrological factor on the bacillary dysentery across the aquatic-terrestrial interface were different for the surface and underground water dynamics. However, all the hydrological factors had the largest impact powers for the three different geographic regions. The baseflow as representing the long-term water dynamic, had the largest impact power on bacillary dysentery in the plain region with the parallel shape river network. The condition inverted in the region with the dendritic pattern river network, that was the quick flow dominated the morbidity. The Huaibei plain region with the parallel shape river network had the majority of bacillary dysentery cases of the whole province. Although the shape of the river network in the Huaibei Plain was a pinnate parallel river network that was more prone to flooding, the rainfall in this area was not much in the province. Combined with the results showing that the quick flow factor had little influence in the plain region, we speculate that the movement of pathogens caused by shallow surface water flow due to relatively gentle slope across the landform was not rapid (Anhui Hydrographic Bureau, 2016); therefore, the increase of suspended matter in the river discharge and the loads of water infrastructure facilities were not large. In contrast, the movement of pathogens caused by long-term dynamic changes in the plain area had a greater impact on the number of patients, possibly due to infiltration rate and local porosity of soil. This is consistent with the finding that there was a lag between the peak of the bacillary dysentery case number and the time of rainfall in Huaibei plain.

In the Jianghuai hilly region, quick flow occupied a dominant position in the incidence of bacillary dysentery. As it is comprised by the parts of the watershed of Yangtze and Huai River, ecological flow of the river discharge and surface runoff nearby the mainstream could involve with a large sediment transport and high turbidity. For the hilly upstream, as the rainfall in this region was between the plain areas and mountains regions of the province, the deeper annual runoff depth and steeper slope's setting than the plain can create a higher river velocity with larger turbulence (Anhui Hydrographic Bureau, 2016). Therefore, we observed that all counties/districts across this hilly region had the greatest influence of the minimum quick flow on bacillary dysentery. This indicated that the surface runoff and interflow in this area, even if the rainfall was not large, could lead a significant health risk to the local population. We speculate that rainstorm-dominated quick flow had a great influence on the movement of pathogens caused by surface scour. This was consistent with the "runoff effect" proposed by researchers, that is, precipitation causes short-term "runoff effect" by flushing pathogens into surface water, re-suspending pathogens in sediments, and making sewage overflow (Levy et al., 2016).

In the rainy mountainous area of Southern Anhui, the influence of the minimum quick flow was the largest similar with that of the Jianghuai Plain region. This showed that even small quick flow of the surface in mountainous areas had the great effect on the health of residents caused by the movement of pathogens. The influence of maximum wind speed and variation range was also large, but the possible mechanism behind it is not clear. The influence of the proportion of urban area in this region was also significant. This may be like the reason that the area ratio of cities in the Jianghuai hills had a greater influence, or it may be due to the drastic change of microclimate. As we known, the impervious surface in urban area increase the surface runoff, and reduces the infiltration rate as well as ground-surface water interaction. Besides, on one hand, the asymptomatic transmission reservoir and higher rates of infection contribute to the incidence pattern in urban areas tended to be more epidemiological than in the rural area (Martinez et al., 2016; White and Greer, 2006). On the other hand, the impact of landscape pattern on the interface between land and water (e.g. water quality) was more complex and multi-scale in urban area

(Shen et al., 2015). Generally, urban land use plays a primary role in degrading water quality in adjacent aquatic systems (Tong and Chen, 2002; White and Greer, 2006). The influences of baseflow and local recharge were smaller than quick flow in this region, suggesting that the long-term influence of groundwater conditions may still influence the bacillary dysentery incidence.

Other meteorological factors, such as the significant influence of temperature on infectious diarrhea, have also been reported (Coffey et al., 2019; Hao et al., 2019; Moors et al., 2013). Temperature has the significant influence on the reproduction and transmission of pathogens, because the pathogen's own survival conditions are closely affected by temperature. In general, there was a positive correlation between temperature and diarrheal diseases, except for viral diarrhea (Levy et al., 2016). One possible explanation for the apparent impact of the temperature range is that there is an optimum temperature range for the diarrheal pathogens (Colston et al., 2019).

4.2. The interactive effects in three different geographical regions maintains robust

From the perspective of interaction effects, the interaction between quick flow, local recharge and baseflow maintains the strong robust correlation in the three geographical regions. There is a consistent synergy between surface and groundwater quality indicators in the same geographical and meteorological characteristics, which indicates the importance of treating surface and groundwater as an integrated hydrology and biogeochemistry (Qiu and Turner, 2015). With the elevation of topographic factors and the change of river network shape, the interaction between quick flow and other non-hydrological factors becomes more and more complex. This trend is also consistent with the province-wide observation that quick flow interacts strongly with non-hydrological factors within the province.

Baseflow and local recharge interact strongly with social, economic and meteorological factors, and the variation trend is not consistent. From the overall trend, baseflow and local recharge mainly interact with many human activity factors in Huaibei plain and Jianghuai hill. However, the acting force of farmland area in Huaibei plain changed from insignificant as a single factor to strong interaction with baseflow and local recharge factors. This phenomenon also occurred in the Jianghuai hill, and the farmland area factor changed from an insignificant single factor to a significant interactive effect. This may be due to agricultural irrigation have diversely impacted the river ecosystems and intensified the water degradation (Levy et al., 2016). As one of the main grain-producing areas in China, low-rain Huaibei and high-rain Jianghuai regions have vast dry land and paddy land, respectively. Since the water withdrawal and irrigation brought by the application of agricultural facilities lead to water losses from the stream, the use and management of such water resources will significantly affect the baseflow regime (Smakhtin, 2001).

In addition, the interactions between urban and water area ratio, baseflow and local recharge are also strong. This may be due to the prevalence of gastrointestinal disease in the surrounding areas of Hefei, the capital city of Anhui province. The region is also home to the province's largest lake, Chaohu Lake. The complex landscape pattern has a strong influence not only on quick flow representing short-term water dynamics, but also on baseflow and local recharge representing long-term water dynamics. The number of health workers and the number of hospital beds representing the level of health resources in the region also changed from the previously insignificant influence to the significant level. The reason for this change may be related to the alteration of the dose-response effect (Levy et al., 2016). Studies have shown that even in places with better sanitation and water treatment facilities, temperature, heavy rainfall and flooding significantly affect the risk of diarrheal disease (Jagai et al., 2015; Morral-Puigmal et al., 2018; N. Zhang et al., 2019).

In the mountainous area of southern Anhui, baseflow, local recharge, quick flow, wind speed and urban area were all single factors with strong impact powers on bacillary dysentery, and their interaction effects were always strong. The incidence of bacillary dysentery in mountainous areas is mainly controlled by the single factors with strong effects, which may be caused by the drastic changes in altitude (Ren et al., 2016; Thompson et al., 2015).

4.3. The scale effects of different factors arose at the provincial level

At the provincial level, population was the most important factor affecting the case number of bacillary dysentery disease, which is consistent with previous studies (Alexander et al., 2018; Martinez et al., 2016; Nichols et al., 2018). The landscape pattern represented by farmland can better explain the incidence of dysentery than the urban distribution, and the influence of other meteorological factors was greater than that of hydrological factors. Although the influence of hydrological factors was significant in the three geographical regions alone, the influence intensity declined at the provincial level. This is probably due to scale (extent) variation, which refers to the overall size of the study area (Turner et al., 1989). Many studies have reported the change in the relationship between landscape pattern and water quality caused by scale variation (Qiu, 2019; Tong and Chen, 2002; Xiao et al., 2016).

In this study, the maximum rainfall and the range of elevation change were not found to have significant influence on bacillary dysentery disease. However, at the provincial scale, the interactive impacts of these two factors changed into significant, which was more consistent with previous studies (Qiu et al., 2019). Thus, objective climate regionalization tools can be combined with observation results to divide broad geographic regions into smaller regions. The homogeneity of the subdivisions in crucial climatic features will facilitate the analysis of driving forces at different scales, and the identification of the route and mechanism of area-specific pathogen transmission will be enhanced (Colston et al., 2019).

The impacts of topographic factors on the bacillary dysentery diseases within the Anhui province was weak. The influence of hydrological factors in the whole province was weak in individual factors and their interactions, but it was always strong in three different geographical regions. It may be because the topography of Anhui province is very different, and different factors further control the transmission route of pathogens in more homogeneous geographical regions. The landscape influences the hydrological process by affecting various physical and chemical processes in the surrounding environment (Qiu et al., 2018; Zipper et al., 2020).

We found that rainfall and average relative humidity as two weak single factors showed a strong interactive impact on bacillary dysentery across the province (q = 0.535). This is inconsistent with the analysis results presented by Colston et al. (2019). They used the Global Land Data Assimilation System (GLDAS) data to carry out cross-scale cohort analysis to study important factors related to rotavirus infection. In stepwise regression analysis, the rainfall factor was eliminated because the interaction between rainfall and relative humidity was not statistically significant. Heavy rain usually increases the risk of diarrhea after a dry period, but decreases it after a wet period. This is produced by alternation of the concentration effect, runoff effect and dilution effect (Levy et al., 2016). The concentration effect indicates that at the low relative humidity condition, the climate is dry enough to allow microbial accumulation in the environment. Although the runoff effect of early rainfall washes out pathogens, the concentration of pathogens is diluted with the increase of continuous rainfall, resulting in reduced exposure risk. Therefore, potential time-dependent mechanisms explaining these interactions between precipitation and the relative humidity.

This study has some limitations; therefore, research findings should be cautiously interpreted when the results are applying other studies. Firstly, although we explore the spatial similarity between various factors and the bacillary dysentery case number in 2015 for counties/cities across three different types of geography areas by applying the reliable Geodetector model, this cross-sectional study could only illustrate the spatial causal relationship in terms of the Tobler's First Law of Geography, that is "everything is usually related to all else but those which are near to each other are more related when compared to those that are further away" (Tobler, 1970). The temporal spatial investigation would further our understanding on the causal relationship between bacillary dysentery and hydrological factors. The comparative studies with longitudinal data could be conducted in the future. Secondly, in terms of the research target, this study explored the direct and the interactive impacts of the hydrological process and bacillary dysentery disease. While hydrological factors could influence infectious diarrhea via various linkages related to the spread and infection of pathogen, this study has not clarified the role of these linkages on the impacts of this water-borne disease. Future research should deeply untangle the mechanism and process of hydrological factors affecting the incidence and spread of bacillary dysentery.

5. Conclusion

Through spatial statistical analysis, our study found that the influence of hydrological factors on the bacillary dysentery disease in Anhui province were the major impact factors in three different geographical regions. Although, the hydrological factors decreased their impact powers at the provincial level. Moreover, the effects of short-term and long-term water dynamics factors varied in different regions. Specifically, in low-rain high-infection Huaibei plain, local recharge and baseflow had larger individual impact powers than quick flow. But quick flow was more important in high-rain low-infection Jianghuai hilly and Wannan mountainous regions. In different geographical regions, hydrological factors maintained strong interactions.

The interactions of quick flow with other non-hydrological factors became more complex with the increase of the elevation and the change of river network shape. Baseflow and local recharge interacted strongly with socioeconomic, meteorological factors, and the variation trend varied in different regions. Our findings revealed the importance of the hydrological factors and provided the clues for better understanding the complex and nonlinear associations between the bacillary dysentery and the risk factors. These findings will support the development of precise public health interventions in reducing bacillary dysentery among high risk geographical areas considering the hydrological effects. The future region scale study could be improved by the comprehensive consideration of the impact factors (e.g. drainage density, dam and spatializable socioeconomic factors) and the accurate location information of the patients which enable the analysis boundary to be the watershed.

CRediT authorship contribution statement

Shudi Zuo: Methodology, Formal analysis, Data curation, Visualization, Writing – original draft, Writing – review & editing. **Lianping Yang:** Conceptualization, Investigation, Data curation, Writing – review & editing, Project administration, Funding acquisition. **Panfeng Dou:** Software, Formal analysis. **Hung Chak Ho:** Methodology, Validation, Writing – review & editing. **Shaoqing Dai:** Methodology, Software, Validation. **Wenjun Ma:** Resources, Writing – review & editing. **Yin Ren:** Writing – review & editing, Supervision, Funding acquisition. **Cunrui Huang:** Writing – review & editing, Supervision, Funding acquisition.

Declaration of competing interest

The authors declare that they have no known competing financial interests or personal relationships that could have appeared to influence the work reported in this paper.

Acknowledgements

Appendix A. Supplementary data

Supplementary data to this article can be found online at https://doi.org/10.1016/j.scitotenv.2020.144609.

References

Alexander, K.A., Heaney, A.K., Shaman, J., 2018. Hydrometeorology and flood pulse dynamics drive diarrheal disease outbreaks and increase vulnerability to climate change in surface-water-dependent populations: a retrospective analysis. PLoS Med. 15, e1002688.

Allen, R.G., Pereira, L.S., Raes, D., Smith, M., 1998. Crop Evapotranspiration-Guidelines for Computing Crop Water Requirements. Food and Agriculture Organization of the United Nations, Rome.

Anhui Climate Center, 2015. 2015 Anhui climate bulletin. URL:. http://www.ahqh.org.cn/ahqhproduct. (Accessed 17 June 2020).

Anhui Hydrographic Bureau, 2016. 2016 Water Resources Bulletin of Anhui Province. Anhui Water Resources Department.

Anhui Provincial Bureau of Statistics, 2016. Anhui statistical yearbook – 2016. URL:. China Statistics Presshttp://tjj.ah.gov.cn/oldfiles/tjj/tjjweb/tjnj/2016/2016.html. (Accessed 17 June 2020).

Anhui Provincial Government, 2013. Anhui province introduction. URL:. http://www.gov.cn/test/2013-03/22/content_2360052.htm. (Accessed 17 June 2020).

Brodie, R.S., Hostetler, S., 2005. A review of techniques for analysing baseflow from stream hydrographs. Presented at the Proceedings of the NZHS-IAH- NZSSS 2005 Conference.

Carlton, E.J., Eisenberg, J.N.S., Goldstick, J., Cevallos, W., Trostle, J., Levy, K., 2014. Heavy rainfall events and diarrhea incidence: the role of social and environmental factors. Am. J. Epidemiol. 179, 344–352.

Coffey, R., Paul, M.J., Stamp, J., Hamilton, A., Johnson, T., 2019. A review of water quality responses to air temperature and precipitation changes 2: nutrients, algal blooms, sediment, pathogens. J. Am. Water Resour. Assoc. 55, 844–868.

Collender, P.A., Morris, C., Glenn-Finer, R., Acevedo, A., Chang, H.H., Trostle, J.A., Eisenberg, J.N.S., Remais, J.V., 2019. Mass gatherings and diarrheal disease transmission among rural communities in Coastal Ecuador. Am. J. Epidemiol. 188, 1475–1483.

Colston, J.M., Zaitchik, B., Kang, G., Peñataro Yori, P., Ahmed, T., Lima, A., Turab, A., Mduma, E., Sunder Shrestha, P., Bessong, P., Peng, R.D., Black, R.E., Moulton, L.H., Kosek, M.N., 2019. Use of earth observation-derived hydrometeorological variables to model and predict rotavirus infection (MAL-ED): a multisite cohort study. Lancet Planet. Health 3, e248–e258.

Dent, B.D., 1999. Cartography: Thematic Map Design. fifth edition. McGraw-Hill, p. 368.

Ding, G., Liu, Q., Jiang, B., Gao, L., Zhang, Y., 2016. Identifying flood-related infectious diseases in Anhui Province, China: a apatial and temporal analysis. Am. J. Trop. Med. Hyg. 94, 741–749.

Fangmeier, D.D., Elliot, W.J., Workman, S.R., Huffman, R.L., Schwab, G.O., 2005. Soil and Water Conservation Engineering. fifth edition. Cengage Learning, p. 528.

GBD 2017 Causes of Death Collaborators, 2018. Global, regional, and national age-sex-specific mortality for 282 causes of death in 195 countries and territories, 1980–2017: a systematic analysis for the Global Burden of Disease Study 2017. Global Health Metrics 392, P1736–P1788.

Gong, L., Hou, S., Su, B., Miao, K., Zhang, N., Liao, W., Zhong, S., Wang, Z., Yang, L., Huang, C., 2019. Short-term effects of moderate and severe floods on infectious diarrheal diseases in Anhui Province, China. Sci. Total Environ. 675, 420–428.

Hamel, P., Valencia, J., Schmitt, R., Shrestha, M., Piman, T., Sharp, R.P., Francesconi, W., Guswa, A.J., 2020. Modeling seasonal water yield for landscape management: applications in Peru and Myanmar. J. Environ. Manag. 270, 110792.

Hao, Y., Liao, W., Ma, W., Zhang, J., Zhang, N., Zhong, S., Wang, Z., Yang, L., Huang, C., 2019. Effects of ambient temperature on bacillary dysentery: a multi-city analysis in Anhui Province, China. Sci. Total Environ. 671, 1206–1213.

IPCC, 2014. Human health: impacts, adaptation, and co-benefits. Climate Change 2014 – Impacts, Adaptation and Vulnerability: Part A: Global and Sectoral Aspects: Working Group II Contribution to the IPCC Fifth Assessment Report. Cambridge University Press, Cambridge URL:. https://www.cambridge.org/core/books/climate-change-2014-impacts-adaptation-and-vulnerability-part-a-global-and-sectoral-aspects/human-health-impacts-adaptation-and-cobenefits/400487C57396C427146921E41E3B27F0. (Accessed 17 June 2020).

Jagai, J.S., Li, Q., Wang, S., Messier, K.P., Wade, T.J., Hilborn, E.D., 2015. Extreme precipitation and emergency room visits for gastrointestinal illness in areas with and without combined sewer systems: an analysis of Massachusetts data, 2003–2007. Environ. Health Perspect. 123, 873–879.

Kraay, A.N.M., Brouwer, A.F., Lin, N., Collender, P.A., Remais, J.V., Eisenberg, J.N.S., 2018. Modeling environmentally mediated rotavirus transmission: the role of temperature and hydrologic factors. Proc. Natl. Acad. Sci. 115, E2782–E2790.

Levy, K., Woster, A.P., Goldstein, R.S., Carlton, E.J., 2016. Untangling the impacts of climate change on waterborne diseases: a systematic review of relationships between diarrheal diseases and temperature, rainfall, flooding, and drought. Environ. Sci. Technol. 50, 4905–4922.

Liu, X., Liu, Z., Zhang, Y., Jiang, B., 2016. Quantitative analysis of burden of bacillary dysentery associated with floods in Hunan, China. Sci. Total Environ. 547, 190–196.

Lo Iacono, G., Armstrong, B., Fleming, L.E., Elson, R., Kovats, S., Vardoulakis, S., Nichols, G.L., 2017. Challenges in developing methods for quantifying the effects of weather and climate on water-associated diseases: a systematic review. PLoS Negl. Trop. Dis. 11, e0005659.

Martinez, P.P., King, A.A., Yunus, M., Faruque, A.S.G., Pascual, M., 2016. Differential and enhanced response to climate forcing in diarrheal disease due to rotavirus across a megacity of the developing world. Proc. Natl. Acad. Sci. 113, 4092–4097.

Mellor, J., Kumpel, E., Ercumen, A., Zimmerman, J., 2016. Systems approach to climate, water, and diarrhea in Hubli-dharwad, India. Environmental Science & Technology 50, 13042–13051.

Milojevic, A., Armstrong, B., Hashizume, M., McAllister, K., Faruque, A., Yunus, M., Kim Streatfield, P., Moji, K., Wilkinson, P., 2012. Health effects of flooding in Rural Bangladesh. Epidemiology 23, 107–115.

Moors, E., Singh, T., Siderius, C., Balakrishnan, S., Mishra, A., 2013. Climate change and waterborne diarrhoea in northern India: impacts and adaptation strategies. Sci. Total Environ. 468-469, S139–S151.

Morral-Puigmal, C., Martínez-Solanas, È., Villanueva, C.M., Basagaña, X., 2018. Weather and gastrointestinal disease in Spain: a retrospective time series regression study. Environ. Int. 121, 649–657.

Nichols, G., Lake, I., Heaviside, C., 2018. Climate change and water-related infectious diseases. Atmosphere 9, 385.

Qiu, J., 2019. Effects of landscape pattern on pollination, pest control, water quality, flood regulation, and cultural ecosystem services: a literature review and future research prospects. Current Landscape Ecology Reports 113–124.

Qiu, J., Turner, M.G., 2015. Importance of landscape heterogeneity in sustaining hydrologic ecosystem services in an agricultural watershed. Ecosphere 6, 1–19.

Qiu, J., Carpenter, S.R., Booth, E.G., Motew, M., Zipper, S.C., Kucharik, C.J., Loheide II, S.P., Turner, M.G., 2018. Understanding relationships among ecosystem services across spatial scales and over time. Environ. Res. Lett. 13, 054020.

Qiu, J., Zipper, S.C., Motew, M., Booth, E.G., Kucharik, C.J., Loheide, S.P., 2019. Nonlinear groundwater influence on biophysical indicators of ecosystem services. Nat. Sustain. 2, 475–483.

Redhead, J.W., May, L., Oliver, T.H., Hamel, P., Sharp, R., Bullock, J.M., 2018. National scale evaluation of the InVEST nutrient retention model in the United Kingdom. Sci. Total Environ. 610-611, 666–677.

Ren, Y., Deng, L.Y., Zuo, S.D., Song, X.D., Liao, Y.L., Xu, C.D., Chen, Q., Hua, L.Z., Li, Z.W., 2016. Quantifying the influences of various ecological factors on land surface temperature of urban forests. Environ. Pollut. 216, 519–529.

Sahle, M., Saito, O., Fürst, C., Yeshitela, K., 2019. Quantifying and mapping of water-related ecosystem services for enhancing the security of the food-water-energy nexus in tropical data–sparse catchment. Sci. Total Environ. 646, 573–586.

Sharp, R., Tallis, H.T., Guerry, A.D., Wood, S.A., Chaplin-Kramer, R., Nelson, E., Ennaanay, D., Wolny, S., Olwero, N., Vigerstol, K., Pennington, D., Mendoza, G., Aukema, J., Foster, J., Forrest, J., Cameron, D., Arkema, K., Lonsdorf, E., Kennedy, C., Verutes, G., Kim, C.K., Guannel, G., Papenfus, M., Toft, J., Marsik, M., Bernhardt, J., Griffin, R., Glowinski, K., Chaumont, N., Perelman, A., Lacayo, M., Mandle, L., Hamel, P., Vogl, A.L., Rogers, L., Bierbower, W., 2015. InVEST 3.2.0 User's Guide.

Shen, Z., Hou, X., Li, W., Aini, G., Chen, L., Gong, Y., 2015. Impact of landscape pattern at multiple spatial scales on water quality: a case study in a typical urbanised watershed in China. Ecol. Indic. 48, 417–427.

Smakhtin, V., 2001. Low flow hydrology: a review. J. Hydrol. 240, 147–186.

Thompson, C.N., Zelner, J.L., Nhu, T.D.H., Phan, M.V., Hoang Le, P., Nguyen Thanh, H., Vu Thuy, D., Minh Nguyen, N., Ha Manh, T., Van Hoang Minh, T., Lu Lan, V., Nguyen Van Vinh, C., Tran Tinh, H., von Clemm, E., Storch, H., Thwaites, G., Grenfell, B.T., Baker, S., 2015. The impact of environmental and climatic variation on the spatiotemporal trends of hospitalized pediatric diarrhea in Ho Chi Minh City, Vietnam. Health & Place 35, 147–154.

Tobler, W., 1970. A computer movie simulating urban growth in the Detroit region. Econ. Geogr. 46, 234–240.

Tong, S.T.Y., Chen, W., 2002. Modeling the relationship between land use and surface water quality. J. Environ. Manag. 66, 377–393.

Turner, M.G., O'Neill, R.V., Gardner, R.H., Milne, B.T., 1989. Effects of changing spatial scale on the analysis of landscape pattern. Landsc. Ecol. 3, 153–162.

Wang, J., Xu, C., 2017. Geodetector: principle and prospective. Acta Geograph. Sin. 72, 116–134.

Wang, J., Li, X., Christakos, G., Liao, Y., Zhang, T., Gu, X., Zheng, X., 2010. Geographical detectors-based health risk assessment and its application in the neural tube defects study of the Heshun region, China. Int. J. Geogr. Inf. Sci. 24, 107–127.

Wang, J., Zhang, T., Fu, B., 2016. A measure of spatial stratified heterogeneity. Ecol. Indic. 67, 250–256.

Wang, Y., Lin, Q., Shi, P., 2018. Spatial pattern and influencing factors of landslide casualty events. J. Geogr. Sci. 28, 259–274.

Wang, H., Di, B., Zhang, T., Lu, Y., Chen, C., Wang, D., Li, T., Zhang, Z., Yang, Z., 2019. Association of meteorological factors with infectious diarrhea incidence in Guangzhou, southern China: a time-series study (2006–2017). Sci. Total Environ. 672, 7–15.

White, M.D., Greer, K.A., 2006. The effects of watershed urbanization on the stream hydrology and riparian vegetation of los Peñasquitos Creek, California. Landsc. Urban Plan. 74, 125–138.

WHO, 2014. Quantitative risk assessment of the effects of climate change on selected causes of death, 2030s and 2050s. URL:. World Health Organizationhttps://apps.who.int/iris/handle/10665/134014. (Accessed 17 June 2020).

Xiao, R., Wang, G., Zhang, Q., Zhang, Z., 2016. Multi-scale analysis of relationship between landscape pattern and urban river water quality in different seasons. Scientific Report 6, 25250.

Yang, L., Liu, C., Bi, P., Vardoulakis, S., Huang, C., 2020. Local actions to health risks of heatwaves and dengue fever under climate change: strategies and barriers among primary healthcare professionals in southern China. Environ. Res. 187, 109688.

Zhang, Y., Bi, P., Hiller, J.E., 2008. Weather and the transmission of bacillary dysentery in Jinan, northern China: a time-series analysis. Public Health Rep. 123, 61–66.

Zhang, F., Liu, Z., Gao, L., Zhang, C., Jiang, B., 2016. Short-term impacts of floods on enteric infectious disease in Qingdao, China, 2005–2011. Epidemiol. Infect. 144, 3278–3287.

Zhang, N., Song, D., Zhang, J., Liao, W., Miao, K., Zhong, S., Lin, S., Hajat, S., Yang, L., Huang, C., 2019a. The impact of the 2016 flood event in Anhui Province, China on infectious diarrhea disease: an interrupted time-series study. Environ. Int. 127, 801–809.

Zhang, J., Sun, Y., Cao, M., Chen, G., 2019b. Analysis of the epidemiological and aetiological characteristics of bacillary dysentery in Anhui Province between 2004 and 2017. Modern Preventive Medicine 46, 1100–1104 (in Chinese).

Zipper, S.C., Jaramillo, F., Wang-Erlandsson, L., Cornell, S.E., Gleeson, T., Porkka, M., Häyhä, T., Crépin, A., Fetzer, I., Gerten, D., Hoff, H., Matthews, N., Ricaurte-Villota, C., Kummu, M., Wada, Y., Gordon, L., 2020. Integrating the water planetary boundary with water management from local to global scales. Earth's Future 8.

Zuo, S., Dai, S., Li, Y., Tang, J., Ren, Y., 2018. Analysis of heavy metal sources in the soil of riverbanks across an urbanization gradient. Int. J. Environ. Res. Public Health 15, 2175.